Environmental Science Advances

ROYAL SOCIETY OF CHEMISTRY

PAPER

View Article Online
View Journal | View Issue

Cite this: *Environ. Sci.: Adv.*, 2024, **3**, 1746

Examining the effectiveness of oiled ballast water treatment processes: insights into hydrocarbon oxidation product formation and environmental implications†

Maxwell L. Harsha, *[a] Danielle E. Verna,[d] Yanila Salas-Ortiz,[a] Ed Osborn,[a] Eduardo Turcios Valle,[a] Aleksandar I. Goranov, [e] Patrick G. Hatcher,[e] Ana M. Aguilar-Islas,[f] Patrick L. Tomco [ag] and David C. Podgorski [abcg]

Ballast water released from ships into coastal environments has been identified as a mechanism that introduces contaminants of concern into coastal ecosystems. This study investigates the treatment processes employed at a ballast water treatment facility in Valdez, Alaska, that remove hydrocarbons from unsegregated ballast water. Specifically, the aim is to quantify and characterize hydrocarbons of emerging concern, known as dissolved hydrocarbon oxidation products (HOPs) and heavy metals (HMs), throughout the treatment process. Specialized analytical techniques were employed, such as non-volatile dissolved organic carbon analysis, fluorescence spectroscopy, Fourier transform-ion cyclotron resonance-mass spectrometry, and inductively coupled plasma triple quadrupole mass spectrometry. Results demonstrate that the treatment removes benzene, toluene, ethylbenzene, and xylene (BTEX) compounds, while HOPs remain. Optical and molecular analyses provide insights into the composition and transformation of HOPs, showing a shift towards more oxygenated and complex compounds during the treatment process. Quantitative analysis of 18 HMs revealed a decrease in the concentration of most dissolved HMs throughout the treatment process, with none exceeding regulatory limits. The findings highlight the need for comprehensive monitoring and regulation of ballast water treatment processes, considering the presence of HOPs and HMs. The results provide valuable insights for environmental monitoring and risk assessment in ballast water treatment, emphasizing the significance of understanding and mitigating the impacts of petroleum derived contaminants on aquatic ecosystems.

Received 5th June 2024
Accepted 5th October 2024

DOI: 10.1039/d4va00187g

rsc.li/esadvances

Environmental significance

The effective treatment of oiled ballast water is crucial to prevent the release of harmful petroleum contaminants into marine ecosystems. Current treatment and monitoring practices focus on a small fraction of volatile hydrocarbons, overlooking two other contaminant classes of concern, dissolved hydrocarbon oxidation products (HOPs) and heavy metals. This study provides novel quantitative and qualitative insights into the transformation of HOPs and dissolved heavy metals at the ballast water treatment at the Valdez Marine Terminal, Alaska. These findings suggest the treatment process is ineffective in removing HOPs, resulting in the discharge of both HOPs and dissolved heavy metals into the aquatic ecosystem from the facility, posing ecological risks and highlighting the need for improved environmental regulations.

1 Introduction

Approximately 10 billion tons of ballast water are transported worldwide annually to stabilize cargo ships during empty voyages between ports.[1] However, the offloading of ballast water raises concerns regarding the transfer of harmful biological agents, such as invasive species and pathogens, as well as the release of chemical contaminants.[2] While the threat of chemical pollution from ballast water offloading decreased with modern double-hulled ships with ballast water tanks segregated from cargo tanks, the North American petroleum industry still faces risks. During winter, ships may require additional ballast water,

[a]*Department of Chemistry, USA. E-mail: mlharsha@uno.edu*
[b]*Chemical Analysis & Mass Spectrometry Facility, USA*
[c]*Pontchartrain Institute for Environmental Sciences, Shea Penland Coastal Education and Research Facility, University of New Orleans, 2000 Lakeshore Drive, New Orleans, Louisiana, USA*
[d]*Prince William Sound Regional Citizens' Advisory Council, Valdez, Alaska, USA*
[e]*Department of Chemistry and Biochemistry, Old Dominion University, 4501 Elkhorn Avenue, Norfolk, Virginia, USA*
[f]*College of Fisheries and Ocean Sciences, University of Alaska Fairbanks, Fairbanks, AK, USA*
[g]*Department of Chemistry, University of Alaska Anchorage, Anchorage, Alaska, USA*

† Electronic supplementary information (ESI) available. See DOI: https://doi.org/10.1039/d4va00187g

which requires storage in unsegregated tanks.[3] Unsegregated ballast water from oil tankers can mix with residual petroleum products, posing a risk of releasing harmful hydrocarbons and oxygen-containing analogues into marine ecosystems. Thus, treatment is necessary before discharging such water into the environment.[4]

Previous studies focused on applying optical spectroscopy to trace the origin of ballast water based on the composition of "natural" dissolved organic matter.[5–9] However, those studies did not examine ballast water in contact with oil. This study focuses on the ballast water treatment facility (BWTF) at the Valdez Marine Terminal in Prince William Sound, Alaska, operated by the Alyeska Pipeline Service Company. Three treatment processes are employed to remove hydrocarbons from unsegregated ballast water: gravity separation, pressurized air flotation treatment, and biological treatment. These techniques utilize physical (separation and volatilization) and biological (oxidation) processes to eliminate hydrocarbons before discharging 1.72 million gallons of effluent daily (average) into Port Valdez, an area of significance for aquaculture and conservation.[10]

In addition to treating ballast water, the BWTF also treats water from other sources. The influent sources are categorized as follows in terms of contribution: stormwater (44%), oiled ballast water (37%), industrial wastewater (14%), and raw water (5%).[10] Stormwater, originating from rain and snowmelt, is the largest influent source and is expected to be uncontaminated, diluting contaminants from other sources.[10] Ballast water is the second largest influent source, primarily responsible for hydrocarbon and metal contamination.[10] The BWTF discharge has been monitored since 1972 by regulatory agencies, including the Environmental Protection Agency and Alaska Department of Environmental Conservation. The Alaska Department of Environmental Conservation currently oversees the facility through the Wastewater Discharge Authorization Program (Alaska Pollutant Discharge Elimination System, permit AK0023248), which mandates monitoring of various parameters in the BWTF effluent, such as flow, pH, total suspended solids, zinc (Zn), total aromatic hydrocarbons, total aqueous hydrocarbons, total recoverable oil and grease, density, dissolved inorganic phosphorus, ammonia, and toxicity.[10] Most recently, the Alaska Department of Environmental Conservation identified zinc, total aromatic hydrocarbons, and whole effluent toxicity as the three primary parameters of concern, most likely to exceed water quality criteria.

Regulating oil contamination levels during the treatment process typically involves measuring the benzene, toluene, ethylbenzene, and xylene (BTEX) family of compounds, also known as total aromatic hydrocarbons.[11] Although BTEX represents only a small fraction of crude oil, it serves as a standard for regulation.[12] Crude oil consists of a complex mixture of compounds with varying molecular weights.[13–15] Higher molecular weight compounds form the unresolved complex mixture and are challenging to characterize and quantify using traditional chromatography techniques this is required for current monitoring methods.[16,17] Furthermore, compounds in crude oil become more polar when oxidized through biotic and abiotic degradation processes.[18–22] The increased polarity from incorporating oxygen heteroatoms further complicates the composition of compounds in the unresolved complex mixture.[23,24] These water-soluble polar hydrocarbon oxidation products (HOPs) can readily partition into the aqueous phase, remaining undetected during transportation from their petroleum source.[13,18,25–33]

The term HOPs was coined by the San Francisco Bay Area Regional Water Quality Control Board (Fry and Steenson, 2019) to clarify the nature of compounds derived from petroleum bodies in petroleum-contaminated groundwater.[34] HOPs are of emerging concern due to their potential risks to the environment.[35,36] Although polycyclic aromatic hydrocarbons are thought to be the drivers of toxicity in vertebrates, Meador and Nahrgang stated, "There are no studies that exist demonstrating that total PAHs are capable of causing toxic effects in early life stage fish at the low levels claimed (0.1–5 $\mu g\ L^{-1}$)".[37] Moreover, there is a mounting body of evidence that some HOPs pose a significant risk to human health and the environment.[27,28,38–56] Additionally, the relationship between the chemical composition of HOPs in the unresolved complex mixture and their toxicity remains to be determined. In the context of ballast water treatment, HOPs may be formed through microbial processes in ballast tanks during transport and within each step of the water treatment process. Although the BWTF process successfully removes BTEX, the impact of the treatment process on the formation of HOPs is unknown. Another emerging concern is the presence of heavy metals (HMs) in ballast water. Despite meeting water quality criteria, whole effluent toxicity testing has revealed chronic toxicity to aquatic organisms in some instances.[10] Dissolved Zn, with its high recorded concentrations in the BWTF effluent, is believed to be the driving parameter for potential toxicity.[10]

This study investigates the concentration and behavior of HOPs and HMs throughout the BWTF treatment process. To achieve this objective, specialized analytical techniques were employed. HOPs were quantified using non-volatile dissolved organic carbon analysis (NVDOC) and characterized *via* fluorescence spectroscopy and Fourier transform-ion cyclotron resonance mass spectrometry. Inductively coupled plasma triple quadrupole mass spectrometry was utilized to determine the quantity of a wide range of HMs. This study serves two purposes: first, to understand the formation and transport of HOPs and HMs through the BWTF process, and second, to quantify and characterize the HOPs and HMs released into Port Valdez through the BWTF discharge. The findings of this study hold significant implications for the functionality and monitoring of the BWTF, as they shed light on two poorly understood and reported classes of contaminants.

2 Materials and methods

2.1. Ballast water treatment facility (BWTF) overview and sample collection

Fig. 1 shows a schematic of the BWTF process. The process starts with the influent being subjected to gravity separation (GS) in large water storage tanks where settling occurs over an

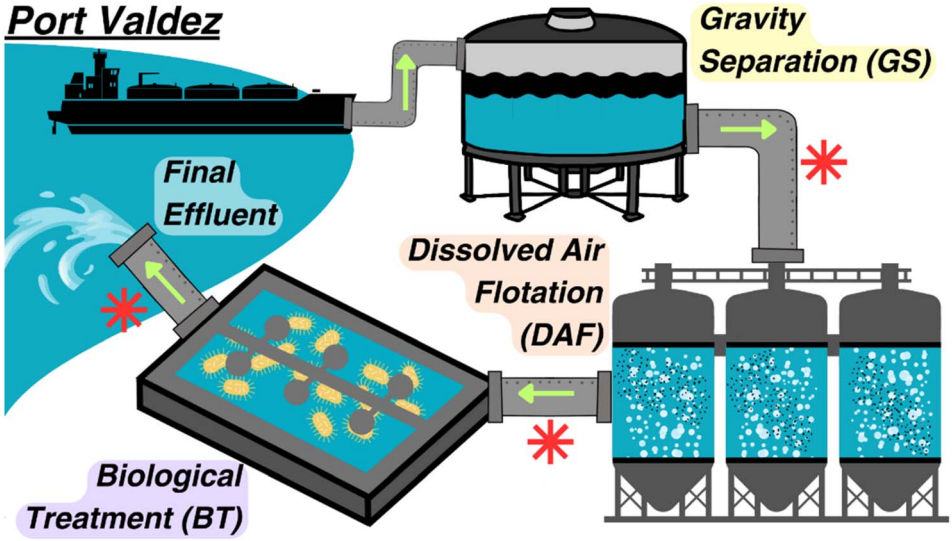

Fig. 1 Overview of the ballast water treatment facility at the Valdez Marine Terminal. Green arrows represent flow direction, and red asterisks represent a sampling point.

average of four hours per each 68.1 million L of water. The oil layer is then skimmed and transferred to a recovery tank, while the water layer proceeds to the dissolved air flotation (DAF) process. In the DAF process, air is bubbled through the oiled water to remove volatile organic compounds, followed by an air stripping process. The generated exhaust vapors are captured and incinerated using regenerative thermal oxidizers. The treated water then passes to the biological treatment (BT) process, where mixing and aeration occur in large open concrete-lined ponds for an average of 16 hours to promote biodegradation. Finally, the treated water is discharged into Port Valdez.

In Fig. 1, the asterisks denote the points at which samples were collected after each treatment. Opportunistic sampling by the Alyeska Pipeline Service Company occurred over one year, resulting in 12 sampling events corresponding to 12 different ballast water offloading events (Table S1†). The sample collection time was staggered at the different process points to ensure that the same ballast water was captured throughout the treatment. A fourth sampling point was added for the last seven sampling events to collect water in the gravity separation tank prior (TP) to ballast offloading to characterize other influent sources (*e.g.* stormwater). Gravity separation tank levels were recorded before and after ballast offloading. Unfiltered samples were collected using 250 mL amber high-density polyethylene (HDPE) bottles and stored at −20 °C until analysis. Thawed samples were subsampled and processed as required for each analysis. The Alyeska Pipeline Service Company provided BTEX measurements for each sample using an Agilent Gas Chromatograph – Model 7890A and Model 7890B.

2.2. Non-volatile dissolved organic carbon (NVDOC) analysis

HOPs were quantified based on NVDOC concentration. Each sample was filtered through a pre-combusted (550 °C > 4 hours) Advantec GF-75 0.3 μm glass fiber filter into a pre-combusted amber glass vial. The pH of each sample was adjusted with ultrapure hydrochloric acid (VWR International) to pH < 2. Samples were analyzed for NVDOC concentration with a Shimadzu TOC-V system equipped with an autosampler. NVDOC was measured as non-purgeable organic carbon converted to CO_2 and detected by a non-dispersive infrared detector.[57] NVDOC was quantified using potassium hydrogen phthalate (VWR International) standards, which were analyzed daily.[58]

2.3. HOPs optical characterization

Ultraviolet-visible and fluorescence excitation–emission matrix (EEM) spectra were utilized to characterize the optical properties of HOPs. The pH of filtered samples was adjusted to pH 8 with NaOH (VWR International) for absorbance and fluorescence measurements with an Aqualog® fluorometer (Horiba Scientific), which measures absorbance and fluorescence simultaneously.[59–61] These optical measurements were carried out in a 1 cm quartz cuvette at an excitation range from 240–800 nm in 5 nm increments and an emission range from 240–800 nm in 2.34 nm increments with an integration period of 5 s. Spectra were blank subtracted and corrected for instrument bias and inner filter effects. Fluorescence intensities were normalized to Raman scattering units before parallel factor analysis, a multiway data analysis technique that decomposes EEMs into several underlying optical signatures.[62] The drEEM toolbox in MATLAB was utilized for parallel factor analysis deconvolution.[62] The spectral components of the resulting statistical model were validated by residual assessment and split-half analysis.[63,64] The validated model was uploaded to the OpenFluor database to compare with published models above 95% similarity score.[65]

Additionally, humification index (HIX) values were determined by the peak area under the emission spectra at 435–480 nm divided by the sum peak area at emission spectra 300–345 and 435–480 nm at excitation 254 nm.[66] Specific UV

absorbance at 254 nm ($SUVA_{254}$) was calculated by dividing the absorbance at 254 nm (in cm^{-1}) by the NVDOC concentration (in mg L^{-1}) × 100 for final SUVA254 units in L mg C^{-1} m^{-1}.

2.4. HOPs molecular composition

Filtered samples were acidified to pH 2 with ultrapure hydrochloric acid (VWR International) and extracted utilizing solid phase extraction (SPE) with Varian Bond Elut PPL cartridges (0.5 g, 3 mL) as reported elsewhere.[67] The final concentrations of the extracts were adjusted to 25 μg C mL^{-1} in 1 : 1 methanol : water (VWR International) to normalize carbon loads across samples to uncover compositional trends. Extracts were analyzed by negative-ion electrospray ionization coupled with a 10 T Apex Qe Fourier transform-ion cyclotron resonance mass spectrometer (Bruker Daltonics) housed in the College of Sciences Major Instrumentation Cluster (COSMIC) facility at Old Dominion University (Norfolk, VA). The instrument was externally calibrated daily with a polyethylene glycol standard, and Suwannee River fulvic acid standard (International Humic Substances Society) was analyzed to evaluate tuning parameters and assess day-to-day variability as Goranov *et al.* 2022 exemplified.[68,69] Collected mass spectra were internally calibrated with naturally abundant fatty acids, dicarboxylic acids, and compounds belonging to the CH_2-homologous series.[70] Calibrated peak lists were refined by removal of blank, salt, doubly-charged, and isotopologue peaks followed by molecular formula assignment (S/N ≥ 3, assignment error ±1 ppm) with elemental criteria ($C_{4-\infty}$, H_{4-200}, O_{1-50}, N_{0-2}, S_{0-1}) utilizing the Toolbox for Environmental Research (TEnvR) in MATLAB.[71] TEnvR default settings were utilized for formula refinement and constraints. Assigned molecular formulae were then classified based on their stoichiometry into the following categories: aromatic (AImod ≥ 0.5), unsaturated low-oxygen (ULO) (AImod < 0.5, H/C < 1.5, O/C < 0.5), unsaturated high-oxygen (UHO) (AImod < 0.5, H/C < 1.5, O/C ≥ 0.5), and aliphatic compounds (H/C ≥ 1.5), with AImod being the modified aromaticity index.[72] The values for each class are their percentage of the total abundance (*i.e.*, % relative abundance).[73]

2.5. Heavy metal quantification

Agilent Technologies 8900 inductively coupled plasma triple quadrupole mass spectrometry system was utilized to measure the concentration of HMs from the BWTF. A 10 mL aliquot of each sample was filtered through 0.45 μm polypropylene syringe filters (Agilent Technologies) and acidified to a concentration of 2% (v/v) trace-metal grade nitric acid (Fisher Scientific) and 0.5% (v/v) trace-metal grade hydrochloric acid (VWR International). The inductively coupled plasma triple quadrupole mass spectrometer was operated in MS/MS mode using helium as the collision gas and ammonia as the reaction gas.[74,75] HMs were quantified based on calibration curves using the environmental calibration standard mix and internal standard mix (Agilent Technologies). The instrument was tuned daily using a solution containing Ce, Co, Li, Mg, Ti, and Y (Agilent Technologies) (1 μg L^{-1}). Specific operating parameters and detection limits are outlined in the ESI (Tables S2 and S3).†

Quantification of dissolved Ni, Cu, and Zn at stations in Prince William Sound and the Gulf of Alaska shelf was done at the University of Alaska Fairbanks by high-resolution inductively coupled plasma mass spectrometry using an Element 2 (ThermoScientific) and isotope dilution. Details on sample collection and processing can be found in Kandel and Aguilar-Islas 2021.[76] Briefly, samples were collected using trace metal clean techniques, filtered through 0.2 μm AcroPak200 filter cartridges (Pall), and acidified to a concentration of 0.2% (v/v) Optima grade nitric acid (Fisher Scientific). Samples were concentrated in-line before analysis using the seaFAST system (Elemental Scientific Inc.).

2.6. Statistical analyses

JMP, Version 17 (SAS Institute Inc.) was used to conduct all statistical analyses. Outliers were eliminated using Cauchy robust outlier analysis. Normality was assessed utilizing the Shapiro–Wilk test. Statistical differences among processing points were evaluated using one-way ANOVA followed by the Tukey–Kramer post hoc test for parametric data, and the Kruskal–Wallis test followed by the Steel-Dwass post hoc test for nonparametric data. Statistical differences in composition between the tank prior (TP) and gravity separation (GS) sampling points were tested using the *t*-test for parametric data and the Mann–Whitney test for nonparametric data. Spearman's rank correlation coefficient (ρ) was utilized to assess the correlation between the characteristics of HOPs and heavy metal concentrations with treatment time and the correlation between assigned molecular formulas and parallel factor analysis components due to the non-linear relationship between variables. Principal component analysis was utilized to examine the variation between the relative contribution of the parallel factor analysis components. The significance level for all statistical analyses was set at $p < 0.05$.

3 Results and discussion

3.1. Hydrocarbon concentrations through the BWTF process

The measured concentrations of BTEX demonstrate that the BWTF process effectively removes these compounds (Fig. 2). BTEX concentrations range from 0.01 ± 0 mg L^{-1} in the effluent to 7.47 ± 1.05 mg L^{-1} after GS (Table S4†). There is a strong negative correlation ($\rho = -0.884$) between BTEX concentration and treatment time, indicating the effectiveness of the BWTF process in reducing BTEX levels. Among the treatment processes, DAF shows the highest efficiency in removing BTEX, as concentrations remain negligible after BT. This result suggests that biodegradation is not a significant factor in removing low concentrations of BTEX from contaminated ballast water. These findings align with previous studies investigating the effectiveness of biodegradation at the BWTF.[11] It is important to note that the measured BTEX levels in the discharge are below the maximum effluent permit limit of 0.73 mg L^{-1} set by the Alaska Department of Environmental Conservation. Moreover, the maximum water quality standard for BTEX in Port Valdez is 0.01 mg L^{-1}, measured at the edge of

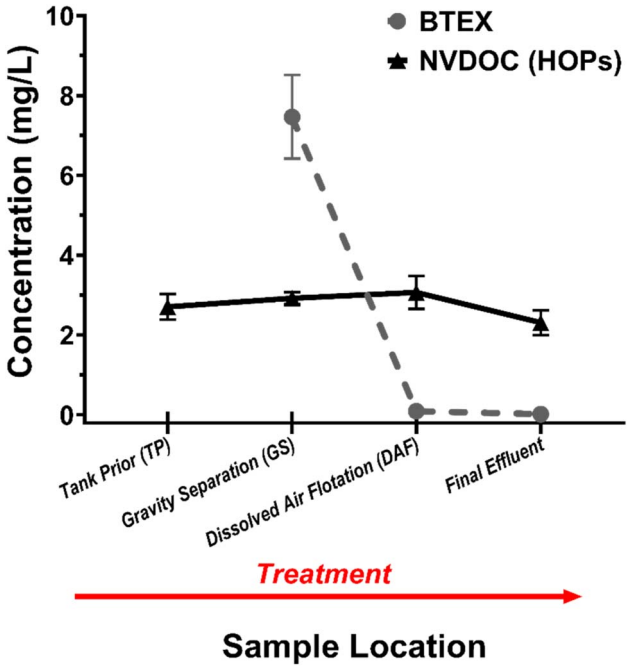

Fig. 2 Changes in the concentration of hydrocarbon oxidation products (HOPs) measured as non-volatile dissolved organic carbon (NVDOC), and benzene, toluene, ethylbenzene, and xylene (BTEX) through treatment process. Samples were collected at each step in the treatment process: Tank Prior (TP) represents wastewater in gravity separation tank prior to ballast offloading, GS after the gravity separation tank, DAF after the dissolved air flotation treatment, final effluent after the biological treatment. The red arrow signifies the order of each step in the treatment process. ($N_{GS,\ DAF,\ final\ effluent} = 12$, $N_{TP} = 7$; ± standard error (SE)).

the BWTF mixing zone.[10] Considering the subsequent dilution of the effluent in Port Valdez (with a dilution factor of 56 : 1 in the mixing zone), the measured BTEX values are well below the maximum water quality limit.

In contrast, there is no statistically significant change in the concentration of dissolved HOPs as measured by NVDOC among the different treatment processes (Fig. 2). The measured NVDOC concentration in the effluent was 2.31 ± 0.31 mg L^{-1}. It is worth noting that the BWTF does not monitor NVDOC levels directly but instead measures total aqueous hydrocarbons, which include BTEX and 16 polycyclic aromatic hydrocarbons to represent the unresolved complex mixture.[10] However, this approach is inaccurate due to additional compounds with varying polarity, which makes the unresolved complex mixture unsuitable for gas-chromatography techniques.[16,17] Currently, there are no specific limits for total aqueous hydrocarbons in the BWTF effluent since it is not considered a parameter of concern. However, the highest measured concentration in the effluent was 0.04 mg L^{-1}.[10] The significant difference (~58-fold) between NVDOC and total aqueous hydrocarbons highlights the complexity of the unresolved complex mixture and the many undetected compounds, suggesting that NVDOC is a more effective technique. Currently, there are no regulatory standards for NVDOC concentration in the BWTF effluent.[10] However, studies demonstrate using NVDOC as an effluent parameter for industrial and municipal treatment processes, providing insight into potentially harmful carbon compounds being released undetected into aquatic ecosystems.[77,78]

3.2. Optical signatures reveal compositional changes in HOPs

Optical analyses reveal changes in the composition of HOPs, providing insights into their source, reactivity, and fate within the BWTF processing. The HIX and specific UV absorbance at 254 nm ($SUVA_{254}$) are optical parameters that indicate molecular size, oxygenation, and aromaticity.[79,80] Increasing HIX values indicate a rise in long-wavelength, oxygenated, and large refractory compounds, while decreasing short-wavelength, small labile compounds. Overall, HIX values increase with BWTF process time ($\rho = 0.659$), ranging from 0.262 ± 0.013 (GS) to 0.376 ± 0.026 (DAF), indicating a compositional shift towards more oxygenated and complex compounds (Table S4†). $SUVA_{254}$ tracks changes in HOPs by measuring light absorption of dissolved organic matter chromophores, with increasing values associated with higher aromaticity. In the BWTF process, $SUVA_{254}$ values range from 0.8 ± 0.1 (effluent) to 1.3 ± 0.1 L mg C^{-1} m^{-1} (TP), but no significant trend with treatment time was observed (Table S5†). These observed HIX and $SUVA_{254}$ values align with previous studies characterizing laboratory-produced HOPs.[81,82] Importantly, they are considerably lower than the values reported for coastal marine natural organic matter (HIX = ~4, $SUVA_{254}$ = ~3), indicating that the source of the dissolved organic matter in the BWTF is petroleum-derived HOPs rather than naturally derived compounds.[83] These findings suggest a transformation of HOPs during the BWTF process, increasing oxygenation and complexity.

Parallel factor analysis was employed to investigate the underlying signatures in the fluorescence EEMs dataset and track the corresponding compositional changes during the BWTF process. A validated four-component parallel factor analysis model was derived (Fig. 3). Each component has specific excitation and emission maxima (Ex/Em) values and exhibits distinct spectroscopic and biogeochemical characteristics. Component 1 (C1) has Ex/Em maxima at 275/295 nm and shows similarity to 15 entries (95–99% similarity score) in the OpenFluor database (containing thousands of component signatures of natural organic matter). The C1 component is called a "protein-like" fluorescence signature in organic biogeochemistry, representing short-wavelength, reactive dissolved organic matter rather than actual proteins. In the context of HOPs, this signature indicates a composition of reduced, aliphatic, and low heteroatom structures, such as 3-ring alkylated and oxygenated polycyclic aromatic hydrocarbons. Component 2 (C2) with Ex/Em values of 250/361 nm matches seven published components (95–97% similarity), including two signatures derived from petroleum. One match is found in a study by Podgorski *et al.*, which investigated petroleum-contaminated groundwater and identified biorefractory HOPs composed of low molecular weight, highly aromatic, and oxygenated compounds.[28] The second match is found in a study

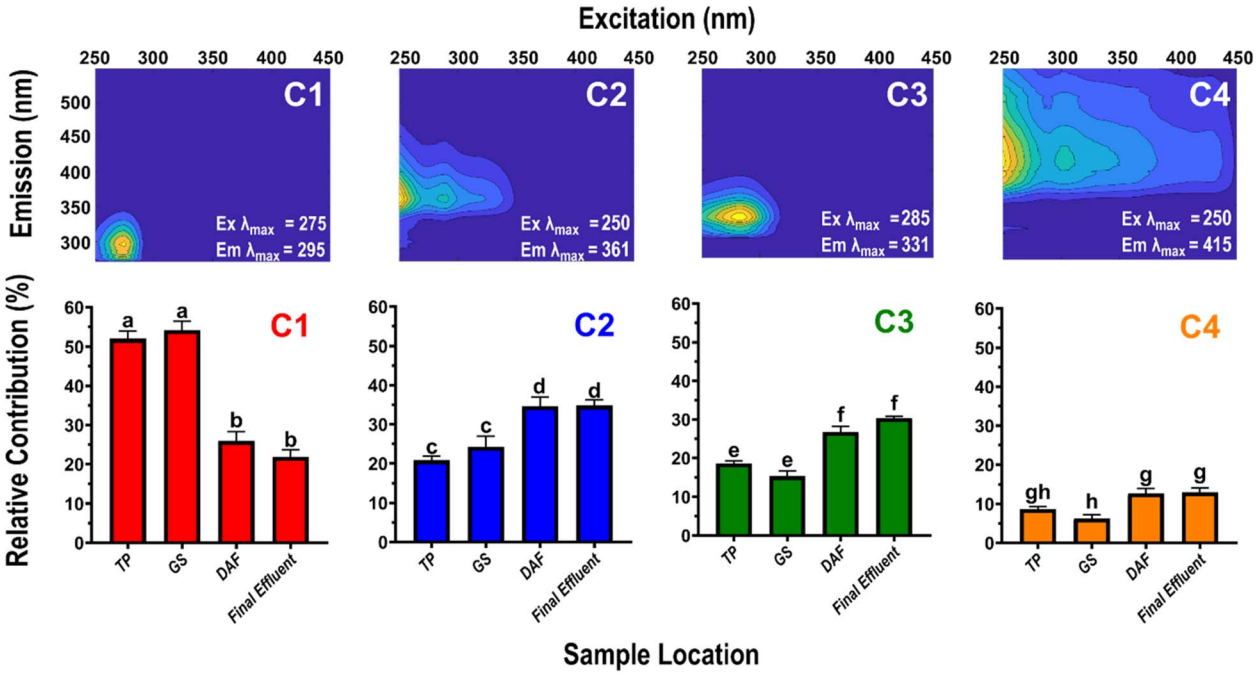

Fig. 3 Validated four-component parallel factor analysis model (top) and relative contributions of *P* parallel factor analysis components (C1–4) (bottom) from fluorescence excitation–emission matrix spectroscopy data of dissolved hydrocarbon oxidation products at various stages of the ballast water treatment process (Tank Prior (TP) represents wastewater in gravity separation tank prior to ballast offloading; GS after the gravity separation tank; DAF after the dissolved air flotation treatment; final effluent after the biological treatment). Connecting letters for each component's relative contribution are multiple comparisons (Steel-Dwass for C1 and C3, Tukey–Kramer for C2 and C4; $p < 0.05$). ($N_{GS,\ DAF,\ final\ effluent} = 12$, $N_{TP} = 7$; ± SE).

by Brünjes *et al.*, focusing on the biodegradation of asphaltenes through laboratory incubations, representing another potential biorefractory signature.[84] Component 3 (C3) with Ex/Em values of 285/331 nm matches 22 published components (96–99% similarity), three of which are petroleum-derived. C3 aligns with C5 in the groundwater study by Podgorski *et al.*, representing short-wavelength, polycyclic aromatic hydrocarbons that are biolabile and acutely toxic.[28] C3 also matches C3 in the asphaltene biodegradation study by Brünjes *et al.*, indicating biolabile and potentially toxic HOPs.[84] Furthermore, C3 matches C4 in a previous study by Harsha *et al.*, which characterized photoproduced HOPs in laboratory simulations, representing reduced, aliphatic HOPs generated from 24 hours irradiated diesel.[81] Component 4 (C4) has Ex/Em values of 250/415 nm and matches 11 published models, including two unique petroleum signatures. C4 corresponds to C4 in the asphaltene biodegradation study by Brünjes *et al.*, exhibiting a "humic-like" fluorescence signature.[84] C4 also matches C1 in a study by Whisenhant *et al.* examining photoproduced HOPs generated from laboratory simulations, where C1 represented the most degraded HOPs that exhibited "humic-like" fluorescence.[82] This result indicates the presence of HOPs composed of long-wavelength, aromatic, oxygenated, and heteroatomic compounds.

Three out of the four components identified in the parallel factor analysis align with components from the Brünjes *et al.* study, suggesting that the optical signatures measured in the BWTF process are likely petroleum-derived.[84] Overall, the HOPs associated with the BWTF process range from short-wavelength (aliphatic, reduced, biolabile) to long-wavelength (aromatic, oxygenated, refractory) compounds, with the order of increasing wavelength being C1 > C3 > C2 > C4.

Principal component analysis (PCA) illustrates the relationship between each component and the treatment process (Fig. 4). C1 closely associates TP and GS data, while C2 is linked to the DAF process. C3 and C4 represent the final effluent. Overall, PCA reveals similarities between TP and GS, as well as between DAF and final effluent data. By measuring the relative contribution of each optical signature, the compositional changes resulting from the BWTF process are uncovered (Fig. 3). There are no significant differences in component contribution between TP and GS and between DAF and the final effluent. Notably, C1 is the only signature that decreases with treatment time ($\rho = -0.797$). This correlation suggests that the short-wavelength HOPs represented by C1 are labile and undergo substantial oxidation during the DAF process, resulting in a ~52% reduction in the C1 signature between GS and DAF. On the other hand, C2, C3, and C4 increase with the amount of time in the BWTF process (ρ = 0.591, 0.743, and 0.567, respectively), indicating that the oxidation process produces varying types of HOPs. After the DAF process, C2 shows an increase of ~43%, the smallest transformation observed among the components coupled, and no compositional change due to BT. This result suggests that C2 may represent more refractory HOPs, as also noted in the matched components in the studies by Podgorski *et al.* and Brünjes *et al.*,

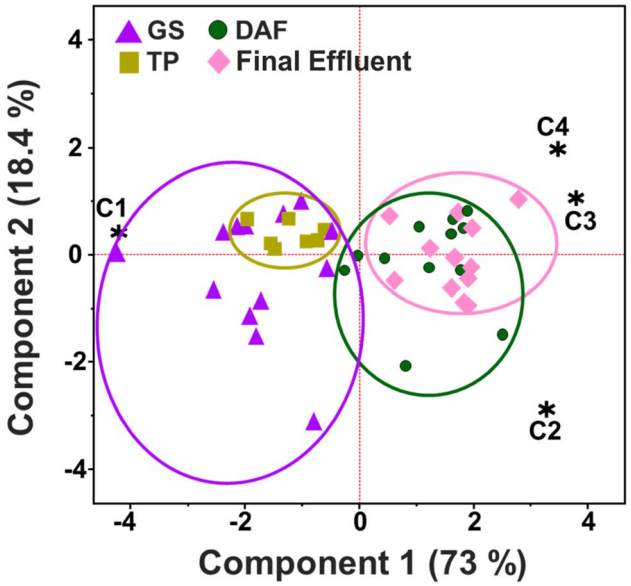

Fig. 4 Principal component analysis (PCA) biplot, loadings represent parallel factor analysis components (C1–4) from fluorescence excitation–emission matrix spectroscopy data of dissolved hydrocarbon oxidation products at various stages of the ballast water treatment process (Tank Prior (TP) represents wastewater in gravity separation tank prior to ballast offloading; GS after the gravity separation tank; DAF after the dissolved air flotation treatment; final effluent after the biological treatment).

indicating C2's potential use for oil treatment and spill monitoring.[28,84] C3 experiences a significant increase of ~74% after DAF and constitutes ~30% of the fluorescence signature observed in the effluent. C4 exhibits an increase of ~104% after DAF treatment and represents the most aromatic and oxygenated signature, reflecting the most degraded HOPs in the BWTF process. Overall, C4 constitutes approximately 10% of the total observed fluorescence at the BWTF, suggesting that the BWTF process does not significantly degrade HOPs into these long wavelength, large molecular weight compounds. Instead, semi-labile/labile HOPs, corresponding to C2 and C3, are released into the ocean, posing a higher likelihood of reactivity and toxicological effects in aquatic ecosystems.

3.3. Molecular composition of HOPs

The molecular composition of HOPs formed during the BWTF was examined using Fourier transform-ion cyclotron resonance mass spectrometry. Overall, the HOPs are mostly composed of unsaturated low-oxygen (ULO) (39.3 ± 3.52–50.5 ± 6.12%) and aliphatic (21.6 ± 5.86–34.3 ± 7.09%) compounds, with smaller contributions of unsaturated high-oxygen (UHO) (13.2 ± 2.97–20.8 ± 3.66%) and aromatic (6.49 ± 1.33–12.5 ± 3.50%) compounds (Fig. 5). Previous studies have indicated that ULO and aliphatic molecular classifications in HOPs contain potentially toxic compounds.[27,40] The high abundance of these compounds at the BWTF poses a potential risk for environmental effects. Positive correlations between assigned molecular formulae classification and parallel factor analysis components reveal molecular markers for each fluorescent signature (Fig. 6). C1 consists predominantly of aliphatic (47.9%) and ULO (39.6%) compositions; C2 consists of aliphatic (30.3%), ULO (31.2%), and UHO (38.5%); C3 is primarily composed of ULO (66.2%) and aromatic (24.6%); and C4 is predominantly composed of ULO (70.8%), aliphatic (15.5%), and aromatic (13.0%) (Fig. 6). These molecular markers align with trends observed in the optical signatures, where aromaticity, oxygenation, and heteroatom content increase with emission wavelength (Table S6†).

A significant increase in CHOS compounds with treatment time was observed ($\rho = 0.422$), indicating that more complex heteroatoms are either formed during or resist the treatment process. Moreover, CHOS compounds may represent surfactants that resist degradation during treatment, as observed previously.[85] The absence of more significant molecular trends with treatment time (Table S5†) is likely attributed to the dependence of HOPs composition on the influent source. Compositional source specificity has been observed in the degradation of naturally dissolved organic matter, with the composition of degradation products remaining source-specific until very late-stage processing.[86,87] Previous studies emphasize this phenomenon in industrial wastewater treatment, where the composition of dissolved organic matter is highly dependent on the influent source and cannot be generalized, as opposed to municipal wastewater and drinking water treatments that have more consistent influent.[88] The molecular composition of HOPs during the BWTF process aligns with this source-specific model, as evidenced by the variability in molecular trends associated with different offloading events (Fig. 7). Each sample set originates from a different influent source, leading to diverse and variable HOPs molecular composition. These findings emphasize the compositional complexity of HOPs while highlighting the utility of optical techniques in measuring bulk compositional changes.

3.4. Trends in heavy metal concentrations

The BWTF process significantly affects the concentration of HMs in oiled ballast water, as revealed by a large quantitative screening of 18 HMs (Ag, Al, As, Ba, Cd, Co, Cr, Cu, Fe, Mn, Mo, Ni, Pb, Sb, Th, U, V, and Zn) with inductively coupled plasma triple quadrupole mass spectrometry. The total heavy metal (THM) concentration decreases significantly with BWTF process time ($\rho = -0.745$). The only significant transformation among treatment stages occurs during the DAF process, where the THM concentration decreases by approximately 34% (Fig. 8). This trend aligns with previous studies identifying the removal of dissolved HMs in wastewater through DAF treatments.[89,90] The measured THM concentrations throughout the BWTF process range from 143 ± 11.0 (final effluent) to 373 ± 29.7 μg L^{-1} (TP). The bulk decrease in HMs does not imply that individual dissolved HMs decrease throughout the process.

Among the 18 HMs measured, 11 display significant trends with BWTF process time. Specifically, Al, V, Cr, Fe, Ni, As, Mo, Pb, and Th exhibit negative correlations, whereas Co and Cu exhibit positive correlations (Table S8†). These significant

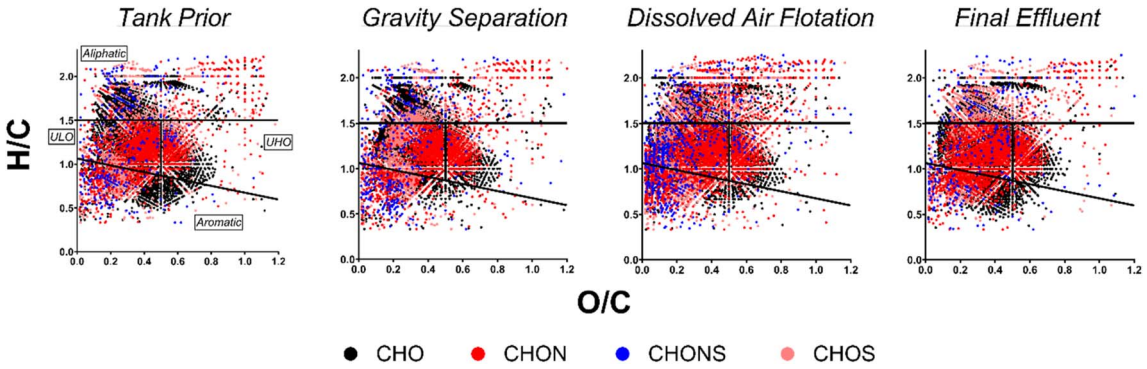

Fig. 5 Van Krevelen plots of the O/C and H/C ratios for molecular formulas assigned to the dissolved hydrocarbon oxidation products at various stages of the ballast water treatment process (tank prior represents wastewater in gravity separation tank prior to ballast offloading; gravity separation after the gravity separation tank; dissolved air flotation after the dissolved air flotation treatment; final effluent after the biological treatment). Data are color-coded by elemental composition. The black lines separate the van Krevelen space into stoichiometric categories: aliphatic, unsaturated low-oxygen (ULO), unsaturated high-oxygen (UHO), and aromatic.

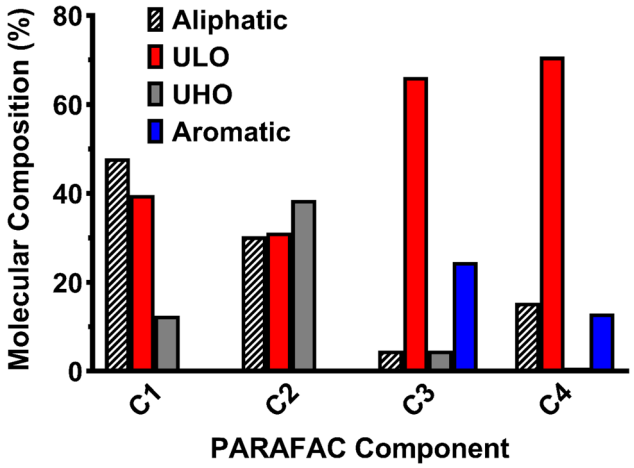

Fig. 6 Molecular composition of each parallel factor analysis component (C1–4).

metals are divided into three concentration levels: high (0.539–203 μg L^{-1}), including Fe, Cu, and Ni; medium (0.148–13.1 μg L^{-1}), including V, As, Al, and Mo; and low (0.038–0.527 μg L^{-1}) including Th, Pb, Cr, and Co (Fig. S2†). Zinc (Zn) is of particular interest, which the Alaska Department of Environmental Conservation categorizes as a parameter of concern and is believed to be the main driver of effluent toxicity due to high measured levels in the discharged effluent.[10] The Zn concentrations in this study range from 30.1 ± 0.139 (TP) to 31.4 ± 0.150 μg L^{-1} (DAF), which are significantly lower than the permit-set limit for effluent (4150 μg L^{-1}) and the water quality standard limit (86.14 μg L^{-1}). The measured effluent Zn concentrations from 2008 to 2017 range from 53 to 1450 μg L^{-1}, with an average of 267 μg L^{-1}, approximately 8.5 times higher than the reported values from this study.[10]

Possible sources of HMs in the oiled ballast water include interactions with metal industrial equipment and from crude oil.[10,91,92] None of the measured HMs exceeded the water quality standards set by the Alaska Department of Environmental Conservation and the Environmental Protection Agency.[10] Levels of Ni, Cu, and Zn were detected in the final effluent (5.69 μg per L Ni, 1.34 μg per L Cu, and 30.3 μg per L Zn) were elevated compared to upper water column (0–100 m) baseline measurements at a downstream station in Prince William Sound (0.31–0.42 μg per L Ni, 0.21–0.42 μg per L Cu, and 0.06–0.49 μg per L Zn), which were similar to upstream levels for these metals over the Gulf of Alaska shelf (0.26–0.28 μg per L Ni, 0.22–0.41 μg per L Cu, and 0.02–0.12 μg per L Zn) (Fig. S3†). These findings suggest that the input of HMs from the BWTF effluent is diminished by dilution and other processes (*e.g.*, biological uptake and particle scavenging) and does not appear to negatively impact the rest of the Sound. However, the impact on the ecosystem near the BWTF would need to be determined. Also, this study cannot determine the fate of dissolved HMs. Still, it is worth noting that if HMs from the effluent are eventually transported to the sediment, the additive accumulation of HMs in sediment poses an ecological risk.[93–95]

3.5. Comparison between stormwater and oiled ballast water

To evaluate the impact of influent sources other than oiled ballast water on contamination levels, measured contaminants were compared between samples taken from the tank prior (TP) to ballast offloading, representing other influent sources, and samples taken following the gravity separation (GS) treatment of oiled ballast water. Since stormwater constitutes the primary influent to the BWTF, TP is assumed to be composed mostly of stormwater and acts as a non-contaminated water source capable of diluting oiled ballast water. Surprisingly, most of the measured data quantifying and characterizing HOPs and HMs were statistically insignificant (Table S9†). Yet, when TP and GS were compared, significant differences in $SUVA_{254}$ and some individual HMs (V, Co, Cu, As, Ag, Pb, Th, U) were observed (Table S9†). A higher $SUVA_{254}$ value in TP (0.013 ± 0.001) suggests the presence of more aromatic compounds in comparison to GS (0.009 ± 0.001). Variability in individual HM concentrations can be attributed to the influence of interaction

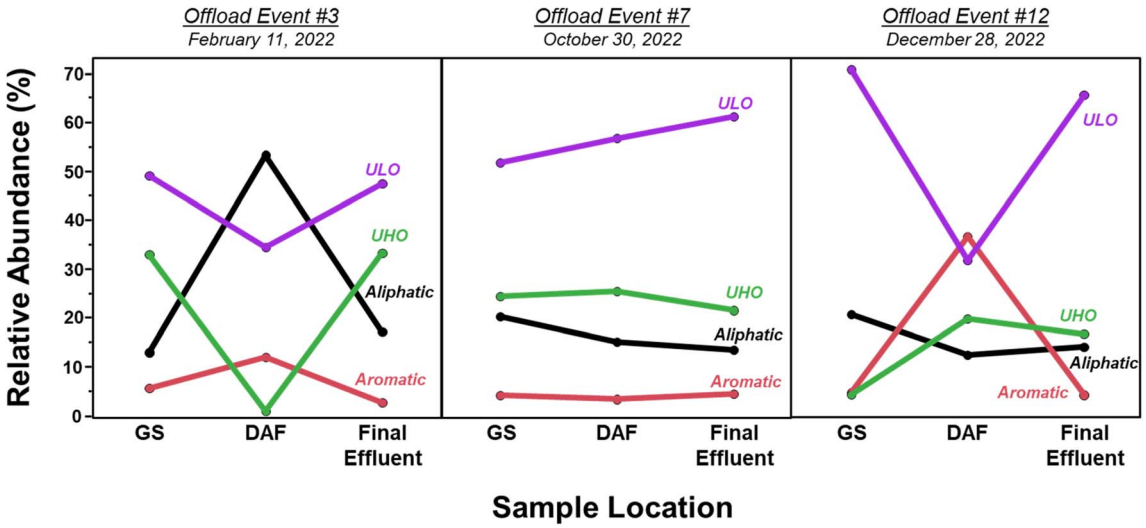

Fig. 7 Variable molecular composition of dissolved hydrocarbon oxidation products at various stages of the ballast water treatment process (GS after the gravity separation tank; DAF after the dissolved air flotation treatment; final effluent after the biological treatment) in three different offloading events. ULO, unsaturated low-oxygen; UHO, unsaturated high-oxygen.

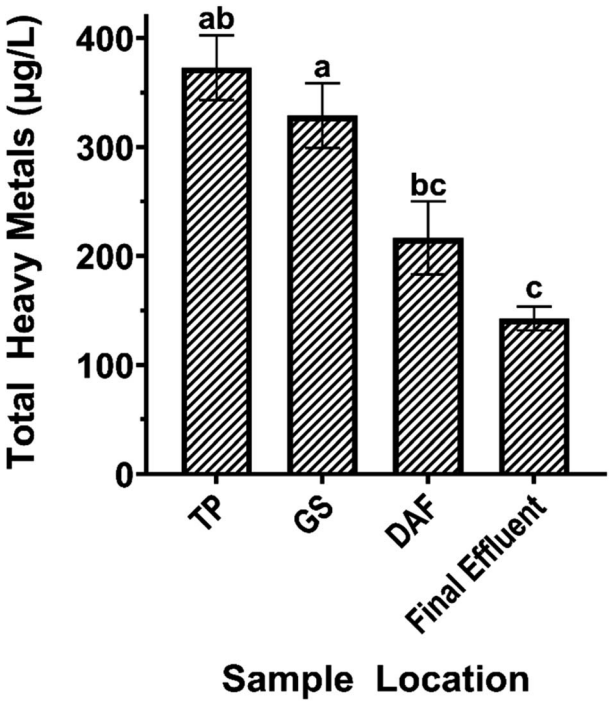

Fig. 8 Shift in concentration of total heavy metals through the treatment process (Tank Prior (TP) represents wastewater in gravity separation tank prior to ballast offloading; GS after the gravity separation tank; DAF after the dissolved air flotation treatment; final effluent after the biological treatment). Connecting letters are Steel-Dwass multiple comparisons ($p < 0.05$). ($N_{GS,final\ effluent} = 12$, $N_{TP} = 7$, $N_{DAF} = 9$; ± SE).

and leaching of metals from industrial equipment, or contribution from natural sources (*e.g.*, atmospheric dust deposition). Based on historical contribution data, these findings challenge the notion that TP is a non-contaminated water source that dilutes contaminants from oiled ballast water.

Recorded values from the gravity separation tank before and after ballast offloading indicate an average dilution factor of 44 : 1 for oiled ballast water. Considering this dilution factor, the expected concentrations and composition of contaminants (HOPs and HMs) were anticipated to be low in TP. However, the actual measurements did not align with these expectations. Previous monitoring data reported very low BTEX levels (below detection limits), suggesting that TP is not contaminated and likely dilutes the contaminants in oiled ballast water.[10] Based on these reports, the NVDOC values in TP samples were expected to be lower. However, the measured NVDOC concentrations suggest that the stormwater may contain hydrocarbons not detected by BTEX measurements. Furthermore, the optical signatures indicate that the source of dissolved organic matter is derived from petroleum rather than naturally occurring substances.

This observed relationship could be attributed to various factors, such as residual oil contamination during the industrial process, higher levels of industrial waste influent, or contaminated stormwater itself. Further research and regular monitoring are necessary to gain valuable insight into the sources of contaminants being retained at TP and then treated at the BWTF. Understanding the composition of the other influents in addition to the ballast water is of utmost importance, especially considering that the Alaska Department of Environmental Conservation permits the discharge of untreated stormwater during periods of high rainfall and snow melt.

3.6. Environmental implications

This study utilized various analytical techniques to investigate the BWTF process in greater detail, uncovering previously undetected contaminants. The findings indicate that the BWTF

effectively removes BTEX from oiled ballast water but fails to remove HOPs. Instead, the process generates and releases diverse compositionally complex HOPs, which may pose ecological risks. The C3 optical signature identified in this study matched other published components known to exhibit acute toxicity. Additionally, potentially toxic molecular classifications (ULO and aliphatic) were highly abundant during the BWTF process. While this study centered on the BWTF in Valdez, Alaska, the treatment techniques utilized (gravity separation, flotation, and biological treatment) are commonly used for treating oiled wastewater.[96] These treatment commonalities suggest that conventional methods are inadequate in effectively treating HOPs, highlighting the necessity for developing alternative treatment approaches for all forms of oiled wastewater.

The toxicity mechanism of HOPs in the environment is not well understood. Still, existing literature suggests that HOPs may be more toxic than their parent petroleum compounds due to increased bioavailability from higher oxygen content.[35] Although the measured levels of HOPs and HMs in the effluent are not alarmingly high, it is crucial to consider the volume of effluent discharged into Port Valdez, which averages 1.72 million gallons per day, with strong seasonal variation.[10] When normalized, this study reveals that 15 kg of HOPs and 11 g of arsenic are released into the water daily during the processing of oiled ballast water. These significant quantities have the potential to enter the aquatic ecosystem, transport through the water column, bioaccumulate in organisms, and sorb into the sediment, posing potential harm over time.

The techniques employed in this study, such as NVDOC and optical analyses, can be used as broad monitoring tools for oil contamination. NVDOC provides a comprehensive quantification of dissolved organic carbon from oiled ballast water, going beyond specific fractions like BTEX or total aqueous hydrocarbons and thus offering insights into carbon release. Additionally, optical signatures can characterize general qualities such as reactivity, aromaticity, and oxygen content. Utilizing remote fluorescence sensors calibrated with petroleum-specific signatures may enable monitoring the formation and transport of HOPs in the BWTF. Adequate monitoring in oiled ballast water treatment is essential for understanding the release and transport of contaminants into the environment.

4 Conclusions

This study examined the treatment processes employed for oiled ballast water at the BWTF in Valdez, Alaska, using various analytical techniques to quantify and characterize HOPs and 18 heavy metals. NVDOC analysis uncovered the BWTF removes regulated BTEX compounds but does not effectively remove HOPs. Instead, optical and molecular analyses reveal a compositional shift in HOPs toward more oxygenated and complex compounds during the treatment process. Moreover, these analyses reveal that the primary composition of HOPs released from the BWTF into Port Valdez is potentially toxic, consisting of fluorescent signature C3 and molecular characteristics of unsaturated low-oxygen and aliphatic compounds. The quantitative screening of several heavy metals (HMs) indicates a decrease in concentration for most dissolved HMs during the treatment process, with none of the concentrations in the final effluent exceeding regulatory limits. Comparing effluent concentrations to those upstream and downstream from the BWTF suggests that the input of discharged HMs does not affect concentrations in Prince William Sound and, consequently, does not impact Gulf of Alaska shelf waters. Findings from this research contribute valuable insights into the challenges and implications of treating oiled ballast water, highlighting the need for enhanced monitoring strategies and treatment techniques to prevent contaminant discharge in aquatic environments.

Data availability

The data supporting this article have been included as part of the ESI.†

Author contributions

Conceptualization: DCP; methodology: MLH, DEV, DCP; formal analysis: MLH, YSO, EO; investigation: MLH, YSO, EO, ETV, AIG, AAI; data curation: MLH, YSO, AIG, AAI; writing – original draft: MLH; writing – review & editing: all authors; resources: DEV, AAI, PGH, PLT, DCP; supervision: DEV, DCP; project administration: MLH, DEV, DCP; funding acquisition: DCP, AAI.

Conflicts of interest

There are no conflicts to declare.

Acknowledgements

Research supported by the Prince William Sound Regional Citizens' Advisory Council (9512.22.01). M. L. Harsha was partially supported by an Oil Spill Recovery Institute Graduate Research Fellowship (22-10-09). Inductively coupled plasma triple quadrupole mass spectrometer awarded through NSF MRI CHE2018417. Heavy metal data from Prince William Sound and the Gulf of Alaska was supported through NSF Grant Number OCE-1656070 to Aguilar-Islas. Thank you to Austin Love at PWSRCAC for the helpful guidance and information. Thanks to Sheila Mann and the Analytical Services Laboratory team at Alyeska Pipeline Service Company for coordination, sample collection, and BTEX analysis.

References

1 V. B. Lamoureux, Organization, W. H., *Guide to Ship Sanitation*, World Health Organization, 1967.
2 S. B. Kurniawan, D. S. A. Pambudi, M. M. Ahmad, B. D. Alfanda, M. F. Imron and S. R. S. Abdullah, Ecological impacts of ballast water loading and discharge: insight into the toxicity and accumulation of disinfection by-products, *Heliyon*, 2022, **8**(3), e09107.

3 A. Love, *2013-2017 Valdez Marine Terminal Water Quality Data Review*, Prince William Sound Regional Citizens' Advisory Council Terminal Operations and Environmental Monitoring Committee, 2018, https://www.pwsrcac.org/document/2013-2017-valdez-marine-terminal-water-quality-data-review/.
4 D. E. Verna and B. P. Harris, Review of ballast water management policy and associated implications for Alaska, *Mar. Pol.*, 2016, **70**, 13–21.
5 K. R. Murphy, G. M. Ruiz, W. T. M. Dunsmuir and T. D. Waite, Optimized Parameters for Fluorescence-Based Verification of Ballast Water Exchange by Ships, *Environ. Sci. Technol.*, 2006, **40**(7), 2357–2362.
6 K. R. Murphy, J. R. Boehme, C. Brown, M. Noble, G. Smith, D. Sparks and G. M. Ruiz, Exploring the limits of dissolved organic matter fluorescence for determining seawater sources and ballast water exchange on the US Pacific coast, *J. Mar. Syst.*, 2013, **111–112**, 157–166.
7 K. Murphy, J. Boehme, P. Coble, J. Cullen, P. Field, W. Moore, E. Perry, R. Sherrell and G. Ruiz, Verification of mid-ocean ballast water exchange using naturally occurring coastal tracers, *Mar. Pollut. Bull.*, 2004, **48**(7), 711–730.
8 M. Noble, G. M. Ruiz and K. R. Murphy, Chemical Assessment of Ballast Water Exchange Compliance: Implementation in North America and New Zealand, *Front. Mar. Sci.*, 2016, **3**, 66.
9 D. H. Carlton, T. Deborah, B. Elizabeth and T. Michael, Optical signatures of seawater and potential use for verification of mid-ocean ballast water exchange, *Mar. Ecol. Prog. Ser.*, 2007, **331**, 35–47.
10 ADEC, A. D. o. E. C., *Alaska Pollutant Discharge Elimination System Permit*, Alyeska Pipeline Service Company, Valdez Marine Terminal, AK0023248, 2019.
11 J. Payne, W. Driskell, J. Braddock and J. Bailey, *Hydrocarbon Biodegradation in the Ballast Water Treatment Facility*, Alyeska Marine Terminal, 2005.
12 B. Hollebone, Chapter 4 – Measurement of Oil Physical Properties, in *Oil Spill Science and Technology*, ed. M. Fingas, Gulf Professional Publishing, Boston, 2011, pp 63–86.
13 G. S. Frysinger, R. B. Gaines, L. Xu and C. M. Reddy, Resolving the Unresolved Complex Mixture in Petroleum-Contaminated Sediments, *Environ. Sci. Technol.*, 2003, **37**(8), 1653–1662.
14 L. C. Krajewski, R. P. Rodgers and A. G. Marshall, 126 264 Assigned Chemical Formulas from an Atmospheric Pressure Photoionization 9.4 T Fourier Transform Positive Ion Cyclotron Resonance Mass Spectrum, *Anal. Chem.*, 2017, **89**(21), 11318–11324.
15 D. C. Palacio Lozano, R. Gavard, J. P. Arenas-Diaz, M. J. Thomas, D. D. Stranz, E. Mejía-Ospino, A. Guzman, S. E. F. Spencer, D. Rossell and M. P. Barrow, Pushing the analytical limits: new insights into complex mixtures using mass spectra segments of constant ultrahigh resolving power, *Chem. Sci.*, 2019, **10**(29), 6966–6978.
16 J. Farrington and J. Quinn, "Unresolved Complex Mixture" (UCM): A brief history of the term and moving beyond it, *Mar. Pollut. Bull.*, 2015, **96**, 29–31.
17 A. M. McKenna, R. K. Nelson, C. M. Reddy, J. J. Savory, N. K. Kaiser, J. E. Fitzsimmons, A. G. Marshall and R. P. Rodgers, Expansion of the Analytical Window for Oil Spill Characterization by Ultrahigh Resolution Mass Spectrometry: Beyond Gas Chromatography, *Environ. Sci. Technol.*, 2013, **47**(13), 7530–7539.
18 C. Aeppli, C. Carmichael, R. K. Nelson, K. L. Lemkau, W. M. Graham, M. C. Redmond, D. L. Valentine and C. M. Reddy, Oil Weathering after the Deepwater Horizon Disaster Led to the Formation of Oxygenated Residues, *Environ. Sci. Technol.*, 2012, **46**, 8799–8807.
19 M. D'Auria, L. Emanuele, R. Racioppi and V. Velluzzi, Photochemical degradation of crude oil: Comparison between direct irradiation, photocatalysis, and photocatalysis on zeolite, *J. Hazard. Mater.*, 2009, **164**(1), 32–38.
20 N. Fry and R. A. Steenson, *User's Guide: Derivation and Application of Environmental Screening Levels (ESLs)*, San Francisco Bay Regional Water Quality Control Board, San Fransisco, 2019, pp 1–35.
21 C. P. Ward, C. M. Sharpless, D. L. Valentine, D. P. French-McCay, C. Aeppli, H. K. White, R. P. Rodgers, K. M. Gosselin, R. K. Nelson and C. M. Reddy, Partial Photochemical Oxidation Was a Dominant Fate of Deepwater Horizon Surface Oil, *Environ. Sci. Technol.*, 2018, **52**(4), 1797–1805.
22 P. Zito, H. Chen, D. C. Podgorski, A. M. McKenna and M. A. Tarr, Sunlight Creates Oxygenated Species in Water-Soluble Fractions of Deepwater Horizon Oil, *J. Hazard. Mater.*, 2014, **280**, 636–643.
23 M. M. Boduszynski, Composition of Heavy Petroleums 1. Molecular-Weight, Hydrogen Deficiency, and Heteroatom Concentration as a Function of Atmospheric Equivalent Boiling-Point up to 1400-Degrees-F (760-Degrees-C), *Energy Fuels*, 1987, **1**(1), 2–11.
24 M. M. Boduszynski, Composition of heavy petroleums. 2. Molecular characterization, *Energy Fuels*, 1988, **2**(5), 597–613.
25 D. H. Freeman and C. P. Ward, Sunlight-driven dissolution is a major fate of oil at sea, *Sci. Adv.*, 2022, **8**(7), eabl7605.
26 H. Maki, T. Sasaki and S. Harayama, Photo-oxidation of biodegraded crude oil and toxicity of the photo-oxidized products, *Chemosphere*, 2001, **44**(5), 1145–1151.
27 P. Zito, D. C. Podgorski, J. Johnson, H. Chen, R. P. Rodgers, F. Guillemette, A. M. Kellerman, R. G. M. Spencer and M. A. Tarr, Molecular-Level Composition and Acute Toxicity of Photosolubilized Petrogenic Carbon, *Environ. Sci. Technol.*, 2019, **53**(14), 8235–8243.
28 D. C. Podgorski, P. Zito, J. T. McGuire, D. Martinovic-Weigelt, I. M. Cozzarelli, B. A. Bekins and R. G. M. Spencer, Examining Natural Attenuation and Acute Toxicity of Petroleum-Derived Dissolved Organic Matter with Optical Spectroscopy, *Environ. Sci. Technol.*, 2018, **52**(11), 6157–6166.

29 D. C. Podgorski, P. Zito, A. M. Kellerman, B. A. Bekins, I. M. Cozzarelli, D. F. Smith, X. Cao, K. Schmidt-Rohr, S. Wagner, A. Stubbins and R. G. M. Spencer, Hydrocarbons to carboxyl-rich alicyclic molecules: A continuum model to describe biodegradation of petroleum-derived dissolved organic matter in contaminated groundwater plumes, *J. Hazard. Mater.*, 2021, **402**, 123998.

30 S. E. M. Dvorski, M. Gonsior, N. Hertkorn, J. Uhl, H. Müller, C. Griebler and P. Schmitt-Kopplin, Geochemistry of Dissolved Organic Matter in a Spatially Highly Resolved Groundwater Petroleum Hydrocarbon Plume Cross-Section, *Environ. Sci. Technol.*, 2016, **50**(11), 5536–5546.

31 A. Islam, A. Ahmed, M. Hur, K. A. Thorn and S. Kim, Molecular-level evidence provided by ultrahigh resolution mass spectrometry for oil-derived DOC in groundwater at Bemidji, Minnesota, *J. Hazard. Mater.*, 2016, **320**, 123–132.

32 K. A. Thorn and G. R. Aiken, Biodegradation of crude oil into nonvolatile organic acids in a contaminated aquifer near Bemidji, Minnesota, *Org. Geochem.*, 1998, **29**(4), 909–931.

33 K. A. Thorn, A. Islam and S. Kim, Characterization of the partial oxidation products of crude oil contaminating groundwater at the U.S. Geological Survey Bemidji research site in Minnesota by elemental analysis, radiocarbon dating, nuclear magnetic resonance spectroscopy, and Fourier transform ion cyclotron resonance mass spectrometry, *Open-File Report 2022–1042*, U.S. Geological Survey, 2022, p. 91, DOI: **10.3133/ofr20221042**.

34 N. Fry and R. A. Steenson, *User's Guide: Derivation and Application of Environmental Screening Levels (ESLs)*, San Francisco Bay Regional Water Quality Control Board, San Fransisco, 2019, pp. 1–35.

35 S. D. Katz, H. Chen, D. M. Fields, E. C. Beirne, P. Keyes, G. T. Drozd and C. Aeppli, Changes in Chemical Composition and Copepod Toxicity during Petroleum Photo-oxidation, *Environ. Sci. Technol.*, 2022, **56**(9), 5552–5562.

36 E. Little, L. Cleveland, R. Calfee and M. Barron, Assessment of the photoenhanced toxicity of a weathered oil to the tidewater silverside, *Environ. Toxicol. Chem.*, 2000, **19**, 926–932.

37 J. P. Meador and J. Nahrgang, Characterizing Crude Oil Toxicity to Early-Life Stage Fish Based On a Complex Mixture: Are We Making Unsupported Assumptions?, *Environ. Sci. Technol.*, 2019, **53**(19), 11080–11092.

38 P. P. Benz, P. Zito, E. Osborn, A. I. Goranov, P. G. Hatcher, M. D. Seivert and W. H. Jeffrey, Effects of burning and photochemical degradation of Macondo surrogate oil on its composition and toxicity, *Environ. Sci.: Processes Impacts*, 2024, **26**(7), 1205–1215.

39 S. M. King, P. A. Leaf, A. C. Olson, P. Zito and M. A. Tarr, Photolytic and Photocatalytic Degradation of Surface Oil from the Deepwater Horizon Spill, *Chemosphere*, 2014, **95**, 415–422.

40 P. Zito, B. A. Bekins, D. Martinović-Weigelt, M. L. Harsha, K. E. Humpal, J. Trost, I. Cozzarelli, L. R. Mazzoleni, S. K. Schum and D. C. Podgorski, Photochemical mobilization of dissolved hydrocarbon oxidation products from petroleum contaminated soil into a shallow aquifer activate human nuclear receptors, *J. Hazard. Mater.*, 2023, **459**, 132312.

41 J. T. McGuire, I. M. Cozzarelli, B. A. Bekins, H. Link and D. Martinović-Weigelt, Toxicity Assessment of Groundwater Contaminated by Petroleum Hydrocarbons at a Well-Characterized, Aged, Crude Oil Release Site, *Environ. Sci. Technol.*, 2018, **52**(21), 12172–12178.

42 Y. He, S. B. Wiseman, X. Zhang, M. Hecker, P. D. Jones, M. G. El-Din, J. W. Martin and J. P. Giesy, Ozonation attenuates the steroidogenic disruptive effects of sediment free oil sands process water in the H295R cell line, *Chemosphere*, 2010, **80**, 578–584.

43 D. Jones, A. G. Scarlett, C. E. West and S. J. Rowland, Toxicity of Individual Naphthenic Acids to Vibrio fischeri, *Environ. Sci. Technol.*, 2011, **45**(22), 9776–9782.

44 H. Peng, J. Sun, H. A. Alharbi, P. D. Jones, J. P. Giesy and S. Wiseman, Peroxisome Proliferator-Activated Receptor γ is a Sensitive Target for Oil Sands Process-Affected Water: Effects on Adipogenesis and Identification of Ligands, *Environ. Sci. Technol.*, 2016, **50**, 7816–7824.

45 A. G. Scarlett, C. E. West, D. Jones, T. S. Galloway and S. J. Rowland, Predicted toxicity of naphthenic acids present in oil sands process-affected waters to a range of environmental and human endpoints, *Sci. Total Environ.*, 2012, **425**, 119–127.

46 S. A. Armstrong, J. V. Headley, K. M. Peru and J. J. Germida, Differences in phytotoxicity and dissipation between ionized and nonionized oil sands naphthenic acids in wetland plants, *Environ. Toxicol. Chem.*, 2009, **28**(10), 2167–2174.

47 S. A. Armstrong, J. V. Headley, K. M. Peru, R. J. Mikula and J. J. Germida, Phytotoxicity and naphthenic acid dissipation from oil sands fine tailings treatments planted with the emergent macrophyte Phragmites australis, *J. Environ. Sci. Health, Part A: Toxic/Hazard. Subst. Environ. Eng.*, 2010, **45**(8), 1008–1016.

48 A. J. Bartlett, R. A. Frank, P. L. Gillis, J. L. Parrott, J. R. Marentette, L. R. Brown, T. Hooey, R. Vanderveen, R. McInnis, P. Brunswick, D. Shang, J. V. Headley, K. M. Peru and L. M. Hewitt, Toxicity of naphthenic acids to invertebrates: Extracts from oil sands process-affected water *versus* commercial mixtures, *Environ. Pollut.*, 2017, **227**, 271–279.

49 A. E. Bauer, R. A. Frank, J. V. Headley, K. M. Peru, A. J. Farwell and D. G. Dixon, Toxicity of oil sands acid-extractable organic fractions to freshwater fish: Pimephales promelas (fathead minnow) and Oryzias latipes (Japanese medaka), *Chemosphere*, 2017, **171**, 168–176.

50 R. A. Frank, R. Kavanagh, B. K. Burnison, G. Arsenault, J. V. Headley, K. M. Peru, G. Van Der Kraak and K. R. Solomon, Toxicity assessment of collected fractions from an extracted naphthenic acid mixture, *Chemosphere*, 2008, **72**, 1309–1314.

51 R. A. Frank, H. Sanderson, R. Kavanagh, B. K. Burnison, J. V. Headley and K. R. Solomon, Use of a (Quantitative) Structure-Activity Relationship [(Q)Sar] Model to Predict

the Toxicity of Naphthenic Acids, *J. Toxicol. Environ. Health, Part A*, 2010, **73**(4), 319–329.

52 K. L. Goff, J. V. Headley, J. R. Lawrence and K. E. Wilson, Assessment of the effects of oil sands naphthenic acids on the growth and morphology of Chlamydomonas reinhardtii using microscopic and spectromicroscopic techniques, *Sci. Total Environ.*, 2013, **442**, 116–122.

53 J. M. Gutierrez-Villagomez, K. M. Peru, C. Edington, J. V. Headley, B. D. Pauli and V. L. Trudeau, Naphthenic Acid Mixtures and Acid-Extractable Organics from Oil Sands Process-Affected Water Impair Embryonic Development of Silurana (Xenopus) tropicalis, *Environ. Sci. Technol.*, 2019, **53**, 2095–2104.

54 S. D. Melvin, C. M. Lanctot, P. M. Craig, T. W. Moon, K. M. Peru, J. V. Headley and V. L. Trudeau, Effects of naphthenic acid exposure on development and liver metabolic processes in anuran tadpoles, *Environ. Pollut.*, 2013, **177**, 22–27.

55 B. A. Bekins, J. C. Brennan, D. E. Tillitt, I. M. Cozzarelli, J. M. Illig and D. Martinović-Weigelt, Biological Effects of Hydrocarbon Degradation Intermediates: Is the Total Petroleum Hydrocarbon Analytical Method Adequate for Risk Assessment?, *Environ. Sci. Technol.*, 2020, **54**(18), 11396–11404.

56 J. E. Schrlau, A. L. Kramer, A. Chlebowski, L. Truong, R. L. Tanguay, S. L. M. Simonich and L. Semprini, Formation of Developmentally Toxic Phenanthrene Metabolite Mixtures by Mycobacterium sp. ELW1, *Environ. Sci. Technol.*, 2017, **51**(15), 8569–8578.

57 A. Stubbins and T. Dittmar, Low volume quantification of dissolved organic carbon and dissolved nitrogen, *Limnol. Oceanogr.: Methods*, 2012, **10**(5), 347–352.

58 B. B. Potter and J. C. Wimsatt, Method 415.3 – Measurement Of Total Organic Carbon, *Dissolved Organic Carbon and Specific Uv Absorbance at 254 Nm in Source Water and Drinking Water*, U. S. Environmental Protection Agency, Washington, DC, 2005.

59 R. G. M. Spencer, L. Bolton and A. Baker, Freeze/Thaw and pH Effects on Freshwater Dissolved Organic Matter Fluorescence and Absorbance Properties from a Number of UK Locations, *Water Res.*, 2007, **41**, 2941–2950.

60 M. M. Tfaily, D. C. Podgorski, J. E. Corbett, J. P. Chanton and W. T. Cooper, Influence of Acidification on the Optical Properties and Molecular Composition of Dissolved Organic Matter, *Anal. Chim. Acta*, 2011, **706**, 261–267.

61 M. Q. Yan, Q. W. Fu, D. C. Li, G. F. Gao and D. S. Wang, Study of the pH Influence on the Optical Properties of Dissolved Organic Matter Using Fluorescence Excitation–Emission Matrix and Parallel Factor Analysis, *J. Lumin.*, 2013, **142**, 103–109.

62 K. R. Murphy, C. A. Stedmon, D. Graeber and R. Bro, Fluorescence Spectroscopy and Multi-Way Techniques. PARAFAC, *Anal. Methods*, 2013, **5**(23), 6557.

63 R. A. Harshman and M. E. Lundy, PARAFAC: Parallel factor analysis, *Comput. Stat. Data Anal.*, 1994, **18**(1), 39–72.

64 C. a. Stedmon and R. Bro, Characterizing Dissolved Organic Matter Fluorescence with Parallel Factor Analysis: A Tutorial, *Limnol Oceanogr. Methods*, 2008, **6**, 572–579.

65 K. R. Murphy, C. A. Stedmon, P. Wenig and R. Bro, OpenFluor – An Online Spectral Library of Auto-Fluorescence by Organic Compounds in the Environment, *Anal. Methods*, 2014, **6**(3), 658–661.

66 T. Ohno, Fluorescence Inner-Fltering Correction for Determining the Humification Index of Dissolved Organic Matter, *Environ. Sci. Technol.*, 2002, **36**, 742–746.

67 T. Dittmar, B. Koch, N. Hertkorn and G. Kattner, A Simple and Efficient Method for the Solid-Phase Extraction of Dissolved Organic Matter (SPE-DOM) from Seawater, *Limnol Oceanogr. Methods*, 2008, **6**(6), 230–235.

68 A. I. Goranov, A. M. Tadini, L. Martin-Neto, A. C. C. Bernardi, P. P. A. Oliveira, J. R. M. Pezzopane, D. M. B. P. Milori, S. Mounier and P. G. Hatcher, Comparison of Sample Preparation Techniques for the (−)ESI-FT-ICR-MS Analysis of Humic and Fulvic Acids, *Environ. Sci. Technol.*, 2022, **56**(17), 12688–12701.

69 J. A. Hawkes, J. D'Andrilli, R. L. Sleighter, H. Chen, P. G. Hatcher, A. Ijaz, M. Khaksan, S. Schum, L. Mazzoleni, R. Chu, N. Tolic, W. Kew, N. Hess, J. Lv, S. Zhang, H. Chen, Q. Shi, R. H. S. Hutchins, D. C. P. Lozano, R. Gavard, H. E. Jones, M. J. Thomas, M. Barrow, H. Osterholz, T. Dittmar, C. Simon, G. Gleixner, S. M. Berg, C. K. Remucal, N. Catalán, R. B. Cole, B. Noreiga-Ortega, G. Singer, N. Radoman, N. D. Schmitt, A. Stubbins, J. N. Agar, P. Zito and D. C. Podgorski, An International Laboratory Comparison of Dissolved Organic Matter Composition by High Resolution Mass Spectrometry: Are We Getting the Same Answer?, *Limnol Oceanogr. Methods*, 2020, 235–258.

70 R. L. Sleighter, G. A. McKee, Z. Liu and P. G. Hatcher, Naturally present fatty acids as internal calibrants for Fourier transform mass spectra of dissolved organic matter, *Limnol. Oceanogr.: Methods*, 2008, **6**(6), 246–253.

71 A. I. Goranov, R. L. Sleighter, D. A. Yordanov and P. G. Hatcher, TEnvR: MATLAB-based toolbox for environmental research, *Anal. Methods*, 2023, **15**(40), 5390–5400.

72 B. P. Koch and T. Dittmar, From Mass to Structure: An Aromaticity Index for High-Resolution Mass Data of Natural Organic Matter, *Rapid Commun. Mass Spectrom.*, 2006, **20**(5), 926–932.

73 J. A. O'Donnell, G. R. Aiken, K. D. Butler, F. Guillemette, D. C. Podgorski and R. G. M. Spencer, DOM Composition and Transformation in Boreal Forest Soils: The Effects of Temperature and Organic-Horizon Decomposition State, *J. Geophys. Res.: Biogeosci.*, 2016, **121**(10), 2727–2744.

74 T. Kubota, *Analysis of Undiluted Seawater Using ICP-MS with Ultra High Matrix Introduction and Discrete Sampling*, Agilent Technologies, Agilent Application Note, 01/25/2022, 2022.

75 W. Proper, E. Mccurdy and J.-i. Takahashi, *Performance of the Agilent 7900 ICP-MS with UHMI for High Salt Matrix Analysis*,

Agilent Technologies, Agilent Application Note, 02/09/2020, 2020.

76 A. Kandel and A. Aguilar-Islas, Spatial and temporal variability of dissolved aluminum and manganese in surface waters of the northern Gulf of Alaska, *Deep Sea Res., Part II*, 2021, **189–190**, 104952.

77 J. W. Park, S. Y. Kim, J. H. Noh, Y. H. Bae, J. W. Lee and S. K. Maeng, A shift from chemical oxygen demand to total organic carbon for stringent industrial wastewater regulations: Utilization of organic matter characteristics, *J. Environ. Manage.*, 2022, **305**, 114412.

78 L. Yang, D. H. Han, B.-M. Lee and J. Hur, Characterizing treated wastewaters of different industries using clustered fluorescence EEM–PARAFAC and FT-IR spectroscopy: Implications for downstream impact and source identification, *Chemosphere*, 2015, **127**, 222–228.

79 J. Gao, C. Liang, G. Shen, J. Lv and H. Wu, Spectral characteristics of dissolved organic matter in various agricultural soils throughout China, *Chemosphere*, 2017, **176**, 108–116.

80 A. Hansen, T. E. C. Kraus, B. Pellerin, J. Fleck, B. D. Downing and B. A. Bergamaschi, Optical properties of dissolved organic matter (DOM): Effects of biological and photolytic degradation, *Limnol. Oceanogr.*, 2016, **61**(3), 1015–1032.

81 M. L. Harsha, Z. C. Redman, J. Wesolowski, D. C. Podgorski and P. L. Tomco, Photochemical formation of water-soluble oxyPAHs, naphthenic acids, and other hydrocarbon oxidation products from Cook Inlet, Alaska crude oil and diesel in simulated seawater spills, *Environ. Sci.: Adv.*, 2023, **2**(3), 447–461.

82 E. A. Whisenhant, P. Zito, D. C. Podgorski, A. M. McKenna, Z. C. Redman and P. L. Tomco, Unique Molecular Features of Water-Soluble Photo-Oxidation Products among Refined Fuels, Crude Oil, and Herded Burnt Residue under High Latitude Conditions, *ACS ES&T Water*, 2022, **2**(6), 994–1002.

83 J. D'Andrilli, V. Silverman, S. Buckley and F. L. Rosario-Ortiz, Inferring Ecosystem Function from Dissolved Organic Matter Optical Properties: A Critical Review, *Environ. Sci. Technol.*, 2022, **56**(16), 11146–11161.

84 J. Brünjes, M. Seidel, T. Dittmar, J. Niggemann and F. Schubotz, Natural Asphalt Seeps Are Potential Sources for Recalcitrant Oceanic Dissolved Organic Sulfur and Dissolved Black Carbon, *Environ. Sci. Technol.*, 2022, **56**(12), 9092–9102.

85 Z. Yuan, C. He, Q. Shi, C. Xu, Z. Li, C. Wang, H. Zhao and J. Ni, Molecular Insights into the Transformation of Dissolved Organic Matter in Landfill Leachate Concentrate during Biodegradation and Coagulation Processes Using ESI FT-ICR MS, *Environ. Sci. Technol.*, 2017, **51**(14), 8110–8118.

86 M. Zark and T. Dittmar, Universal molecular structures in natural dissolved organic matter, *Nat. Commun.*, 2018, **9**(1), 3178.

87 D. C. Podgorski and B. A. Bekins, Comment on "Complex mixture toxicology: Evaluation of toxicity to freshwater aquatic receptors from biodegradation metabolites in groundwater at a crude oil release site, recent analogous results from other authors, and implications for risk management", *Aquat. Toxicol.*, 2023, **265**, 106744.

88 W. Shi, W.-E. Zhuang, J. Hur and L. Yang, Monitoring dissolved organic matter in wastewater and drinking water treatments using spectroscopic analysis and ultra-high resolution mass spectrometry, *Water Res.*, 2021, **188**, 116406.

89 H. Al-Zoubi, K. A. Ibrahim and K. A. Abu-Sbeih, Removal of heavy metals from wastewater by economical polymeric collectors using dissolved air flotation process, *J. Water Proc. Eng.*, 2015, **8**, 19–27.

90 G. Pooja, P. S. Kumar, G. Prasannamedha, S. Varjani and D.-V. N. Vo, Sustainable approach on removal of toxic metals from electroplating industrial wastewater using dissolved air flotation, *J. Environ. Manage.*, 2021, **295**, 113147.

91 M. A. Ajeel, A. A. Ajeel, A. M. Nejres and R. A. Salih, Assessment of Heavy Metals and Related Impacts on Antioxidants and Physiological Parameters in Oil Refinery Workers in Iraq, *J. Health Pollut.*, 2021, **11**(31), 210907.

92 E. Chinedu and C. K. Chukwuemeka, Oil Spillage and Heavy Metals Toxicity Risk in the Niger Delta, Nigeria, *J. Health Pollut.*, 2018, **8**(19), 180905.

93 A. M. Iordache, C. Nechita, R. Zgavarogea, C. Voica, M. Varlam and R. E. Ionete, Accumulation and ecotoxicological risk assessment of heavy metals in surface sediments of the Olt River, Romania, *Sci. Rep.*, 2022, **12**(1), 880.

94 L. S. Miranda, G. A. Ayoko, P. Egodawatta and A. Goonetilleke, Adsorption-desorption behavior of heavy metals in aquatic environments: Influence of sediment, water and metal ionic properties, *J. Hazard. Mater.*, 2022, **421**, 126743.

95 Y. Zhao, Y. Yang, R. Dai, S. Leszek, X. Wang and L. Xiao, Adsorption and migration of heavy metals between sediments and overlying water in the Xinhe River in central China, *Water Sci. Technol.*, 2021, **84**(5), 1257–1269.

96 A. D. L. M. de Medeiros, C. J. G. d. Silva Junior, J. D. P. d. Amorim, I. J. B. Durval, A. F. d. S. Costa and L. A. Sarubbo, Oily Wastewater Treatment: Methods, Challenges, and Trends, *Processes*, 2022, **10**(4), 743.